Journal of Chromatography, 590 (1992) 3–15
Elsevier Science Publishers B.V., Amsterdam

CHROMSYMP. 2385

Theory of optimization of ideal displacement chromatography of binary mixtures

S. C. David Jen and Neville G. Pinto*

Department of Chemical Engineering, University of Cincinnati, Cincinnati, OH 45221-0171 (USA)

ABSTRACT

The optimization of the displacement chromatographic separation of binary mixtures for maximizing the column throughput was investigated. The theory of coherence, based on the compound Langmuir model, was used to establish the general behavior of displacement chromatography through the use of distance–time diagrams. It is shown that columns should be operated at their resolution point for maximum throughput, and this is applicable to non-ideal displacement chromatography. Concentration of the feed sample to an optimum value is necessary to maximize the column throughput. The effects of the separation factor, capacity factors and resin saturation capacity with respect to throughput were also investigated. An analysis of the displacer affinity showed that low-affinity displacers are generally desirable in terms of development, regeneration and solubility requirements. A simple method is proposed for determining the optimum column loading for a given separation, and the extension of this approach to multi-component mixtures is discussed. This method can be used for the optimization of displacement separations of systems approximated by the compound Langmuir model.

INTRODUCTION

As the commercialization of biotechnology progresses, the need to develop cost-effective downstream processing strategies is becoming more intense [1]. Chromatographic purification steps, normally the most expensive steps, are therefore prime targets for reducing costs. Most current applications of preparative chromatography have used overloaded elution chromatography. It is known that preparative elution chromatography suffers from several drawbacks, including peak tailing, diluted product and low column loading [2]. In contrast, displacement chromatography provides several advantages, such as concentrated products, high column loading and low solvent consumption. Recently, progress in displacement chromatography for preparative applications, especially bioseparations, has been notable [2,3]. However, displacement chromatography is not yet widely accepted in downstream processing. There are several obstacles that hamper the application of this technique: lengthy regeneration, toxic displacers [4], low operational flow-rates [5] and complex method development and optimization [6]. Problems of regeneration and toxic displacers were recently addressed for ion-exchange displacement chromatography for protein purifications [7,8]. Novel support materials that enhance mass transfer through convective flow in the pores [9] may provide a solution to low operational flow-rates.

Method development and optimization of displacement chromatography are complicated by operation in the non-linear region of the isotherm and the use of displacers for achieving the separation. For chromatographic separations in elution mode, the fundamental resolution equation,

$$R_s = \frac{\sqrt{N}}{4} \cdot \frac{\alpha - 1}{\alpha} \cdot \frac{k_i' + 1}{k_i'} \qquad (1)$$

has been used to establish guidelines for optimizing the resolution and the throughput in both the analytical and preparative modes [10,11]. However, eqn. 1 is not applicable to the optimization of displacement chromatography. Further, the most important parameter in preparative-scale separations, the column loading, can only be optimized

with a non-linear theory of chromatography. Previous approaches to optimizing displacement chromatography have used non-ideal chromatographic models to simulate specific separations [6,12,13]. Although these approaches predict the effects of axial dispersion and mass transfer rates, they cannot provide an overall picture of the dynamics of the displacement development process in a concise form, an essential component for a simple optimization technique. Distance–time diagrams [14] based on the theory of multi-component chromatography can provide such a tool for the efficient description of the chromatographic processes and at the same time be applicable to the cases where axial dispersion and mass transfer rates are important [15].

In this study, an optimization method based on the coherence theory of multi-component chromatography [14] was developed. The coherence theory assumes ideal chromatographic behavior, and uses the compound Langmuir model for representing multi-component equilibrium behavior. A key feature of this model is that it provides a mathematical transformation, the *h*-transformation, for depicting the dynamics of propagating systems, such as displacement development, in simple terms. The coherence theory has already been applied to displacement chromatography [2,14,16], and equations in terms of *h* compositions for calculating various resolution points are available for both systems involving stoichiometric [14] and non-stoichiometric adsorption behavior [2]. However, these equations have not been exploited for optimizing the displacement process. In this work, a framework has been developed for optimizing ideal displacement chromatography of binary mixtures. Analytical expressions in terms of mobile phase concentrations for displacement chromatography have been developed for the general case of non-stoichiometric adsorption, and effects of operating and thermodynamic parameters have been evaluated. Further, it has been shown that finite mass transfer rates do not alter optimal operating conditions identified with the coherence model.

The coherence approach to modeling displacement chromatography has been successful in several cases. For example, concentration profiles for the displacement chromatography of a fifteen-component rare earth mixture have been correctly calculated using the *h*-transformation [17], and the coherence model has been demonstrated to describe adequately displacement development in a high-performance liquid chromatographic system [18]. It has also been shown that a semi-ideal model [19] based on the compound Langmuir isotherm model predicted well the band profiles obtained earlier for the formation of the isotachic train. Further, for overloaded elution chromatography it has been demonstrated that optimum conditions identified with an ideal model are applicable to non-ideal cases, with minor modifications [15]. These results indicate that the development of an optimization model based on the compound Langmuir isotherm and ideal chromatographic behavior is likely to be practically useful. However, it must be emphasized that for systems that cannot be approximated by the compound Langmuir isotherm, such as systems that show selectivity reversal [20,21], the optimization method will have limited utility.

As the method developed is restricted to systems obeying the compound Langmuir isotherm, caution has to be exercised in using the coefficients of this isotherm. It has been shown that the use of single-component Langmuir coefficients in the compound Langmuir isotherm violates the Gibbs–Duhem relationship, unless the column saturation capacities are equal for all components [22,23]. For the chromatography of molecules of widely different size, such an assumption is unrealistic. Cox and Snyder [24] have reported significant effects of different column saturation capacities on overloaded elution chromatography. Nevertheless, if the compound Langmuir model is considered as a mathematical rather than a physical model, the use of different column saturation capacities becomes acceptable [25]. Further, the compound Langmuir model, based only on simple kinetic considerations, accounts only for competitive adsorption behavior. Hence, the use of single-component coefficients, although widely practised, is not recommended. Multi-component Langmuir coefficients can be conveniently measured with chromatographic methods [26,27], and these are recommended for use with the optimization procedure.

THEORY AND METHOD

Coherence theory

The coherence theory of chromatography [14] is based on the multi-component Langmuir isotherm. In terms of the elution capacity factor, k'_i, this isotherm takes the form

$$Q_i^* = \frac{k'_i c_i}{1 + \sum_{j=1}^{n} b_j c_j} \qquad i = 1, \ldots, n \tag{2}$$

When used with the coherence theory, the species in eqn. 2 are numbered according to their affinity for the stationary phase, with component i having a stronger affinity than component $i + 1$. Hence for displacement the displacer is component 1.

The coherence theory is most useful when compositions are expressed in an orthogonalized composition space called the h space [14]. The transformation from the c composition space to the h space involves the calculation of the roots of the equation

$$\sum_{i=1}^{n} \frac{b_i c_i}{h \cdot \dfrac{k'_i}{k'_1} - 1} = 1 \tag{3}$$

For systems involving trivial roots, these roots are obtained from

$$h_{j-1} = \frac{k'_1}{k'_j} \text{ or } h_j = \frac{k'_1}{k'_j} \text{ if } c_j = 0 \ (1 < j \leqslant n) \tag{4}$$

$$h_1 = 1 \quad \text{if} \quad c_1 = 0$$

In the h space, the adjusted composition velocity for a boundary with the jth root as the variable root is

$$U_j = h_j \prod_{i=1}^{n} h_i \prod_{i=1}^{n} \alpha_{i1} \tag{5}$$

where

$$\alpha_{i1} = k'_i / k'_1 \tag{6}$$

Real velocities can be calculated from adjusted velocities as follows

$$u_j = \frac{u_0}{1 + \dfrac{k'_{n+1}}{U_j}} \tag{7}$$

Column throughput: equation derivation

A distance–time diagram for displacement chromatography of a binary mixture can be generated from wave velocities (eqn. 5) calculated from the h compositions of the presaturant, feed and displacer solutions [14]. For a binary separation of components 2 and 3 using a displacer 1, a simplified distance–time diagram is shown in Fig. 1. Nine waves are generated and all these waves are sharp if

$$h'_3 < 1 + b_1 c_1^{\mathrm{f}} \tag{8}$$

The adjusted time, τ, in Fig. 1 is defined as [14]

$$\tau = \frac{t}{k'_4} \cdot u_0 \tag{9}$$

Adjusted velocities for each wave can be obtained from eqn. 5 as

$$U_1 = \alpha_{42} (1 + b_2 c_2^{\mathrm{f}} + b_3 c_3^{\mathrm{f}}) \tag{10}$$

$$U_2 = \alpha_{41} h'_3 \tag{11}$$

$$U_3 = \alpha_{41} (1 + b_1 c_1^{\mathrm{f}}) = U_8 = U_9 \tag{12}$$

$$U_4 = \alpha_{41} h'_2 \alpha_{21} (1 + b_1 c_1^{\mathrm{f}}) \tag{13}$$

$$U_5 = \alpha_{41} (1 + b_1 c_1^{\mathrm{f}})(1 + b_2 c_2^{\mathrm{f}} + b_3 c_3^{\mathrm{f}}) \tag{14}$$

$$U_6 = \alpha_{41} h'_2 \alpha_{31} (1 + b_1 c_1^{\mathrm{f}}) \tag{15}$$

$$U_7 = \alpha_{41} h'_3 \alpha_{31} (1 + b_1 c_1^{\mathrm{f}}) \tag{16}$$

The h-roots in eqns. 11, 13, 15 and 16 can be related to the equilibrium data and the feed composition

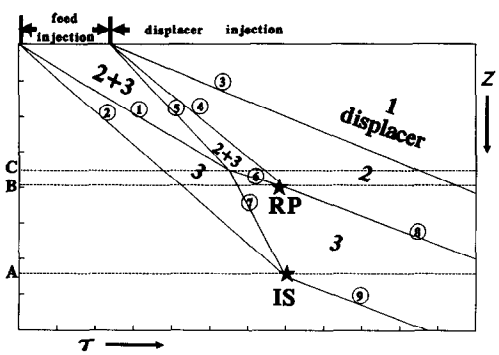

Fig. 1. Simplified distance–time diagram for the displacement chromatography of binary separations. The numbers in the circles represent the wave number.

$$h'_2 = \tfrac{1}{2}\left(\alpha_{13}(1 + b_3c_3^f) + \alpha_{12}(1 + b_2c_2^f) - \{[\alpha_{13}(1 + b_3c_3^f) - \alpha_{12}(1 + b_2c_2^f)]^2 + 4\alpha_{12}\alpha_{13}b_2c_2^f b_3c_3^f\}^{\frac{1}{2}}\right) \quad (17)$$

$$h'_3 = \tfrac{1}{2}\left(\alpha_{13}(1 + b_3c_3^f) + \alpha_{12}(1 + b_2c_2^f) + \{[\alpha_{13}(1 + b_3c_3^f) - \alpha_{12}(1 + b_2c_2^f)]^2 + 4\alpha_{12}\alpha_{13}b_2c_2^f b_3c_3^f\}^{\frac{1}{2}}\right) \quad (18)$$

Eqns. 10 and 14 can be used to calculate the coordinates of the first interference point, where wave 5 catches wave 1:

$$\tau_{15} = \frac{U_5}{U_5 - U_1} \cdot \tau_{feed} \quad (19)$$

and

$$z_{15} = \tau_{15} U_1 = \frac{U_1 U_5}{U_5 - U_1} \cdot \tau_{feed} \quad (20)$$

Similarly, eqns. 13, 15, 19 and 20 give the second interference point, where wave 4 catches wave 6:

$$\tau_{46} = \frac{\dfrac{U_5 (U_6 - U_1)}{U_5 - U_1} - U_4}{U_6 - U_4} \cdot \tau_{feed} = \tau^{RP} \quad (21)$$

and

$$z_{46} = U_4\left[\frac{\dfrac{U_5(U_6 - U_1)}{U_5 - U_1} - U_4}{U_6 - U_4} - 1\right]\tau_{feed} = z^{RP} \quad (22)$$

At this point the complete separation of components 2 and 3 is first achieved. This is defined as the resolution point (RP point in Fig. 1), and is indicated with the coordinates τ^{RP} and z^{RP} in eqns. 21 and 22. Note that the resolution point occurs whether or not eqn. 8 is satisfied.

Define a dimensionless time, θ, as:

$$\theta = \frac{t}{L} \cdot u_0 = \frac{t}{t_0} \quad (23)$$

In terms of θ, a resolution capacity θ^{RP}_{feed} is defined as the maximum feed time for which the resolution of the binary mixture can be achieved within a column length L. The resolution capacity can be calculated by substituting eqns. 9–16 and 23 into eqn. 22 and letting $L = z_{RP}$:

$$\theta^{RP}_{feed} = \frac{1 - \alpha_{32}}{1 + b_2c_2^f + b_3c_3^f - \alpha_{31}h'_2}(k'_2 - K'_1) \quad (24)$$

where $\alpha_{31}h'_2$ is only a function of properties of components 2 and 3. Therefore, the term outside the parentheses on the right-hand side of eqn. 24 is only a function of the properties and compositions of components 2 and 3. K'_1 is the frontal capacity factor of pure displacer, and can be directly measured experimentally from frontal chromatography of the displacer by

$$K'_1 = \frac{k'_1}{1 + b_1c_1^f} = \frac{T_1 - T_0}{T_0} \quad (25)$$

where T_1 is the breakthrough time of the displacer. In order to locate the isotachic point, the point beyond which all wave velocities are equal, it is necessary to locate the third interference point, where wave 7 catches wave 2 (Fig. 1). If eqn. 8 is satisfied, it can be shown from eqns. 11, 16 and 19–22 that

$$\tau_{27} = \frac{U_7 - U_1}{U_7 - U_2} \cdot \frac{U_5}{U_5 - U_1} \cdot \tau_{feed} = \tau^{IS} \quad (26)$$

and

$$z_{27} = \frac{U_7 - U_1}{U_7 - U_2} \cdot \frac{U_2 U_5}{U_5 - U_1} \cdot \tau_{feed} = z^{IS} \quad (27)$$

If eqn. 8 is not satisfied, explicit equations cannot be derived for the isotachic coordinates. Analogous to the resolution capacity, an isotachic capacity, θ^{IS}_{feed}, can be defined as the maximum feed time for which the isotachic condition can be achieved within a column length L. The isotachic capacity can be calculated from eqn. 27 as

$$\theta^{IS}_{feed} = \frac{\left(1 - \dfrac{K'_1}{k'_2}\right)\left(1 - \dfrac{k'_3}{K'_1}\right)}{\dfrac{1 + b_2c_2^f + b_3c_3^f}{k'_2} - \dfrac{\alpha_{31}h'_3}{K'_1}} \quad (28)$$

It can also be shown from eqn. 12 that once the isotachic point is reached, the concentrations of components 2 and 3 are

$$c_2^{IS} = \frac{\alpha_{21}(1 + b_1c_1^f) - 1}{b_2} = \frac{\dfrac{k'_2}{K'_1} - 1}{b_2} \quad (29)$$

and

$$c_3^{IS} = \frac{\alpha_{31}(1 + b_1 c_1^f) - 1}{b_3} = \frac{\frac{k'_3}{K'_1} - 1}{b_3} \quad (29)$$

The band width for the zone of pure component 2, $\Delta\tau_{34}$, for the case when the resolution point is not attained in the column, $\theta_{feed} > \theta_{feed}^{RP}$, is given by

$$\Delta\tau_{34} = (\tau - \tau_{feed})\left(1 - \frac{U_3}{U_4}\right) \quad (30)$$

or, in terms of dimensionless time,

$$\Delta\theta_{34} = K_1\left(1 - \frac{\alpha_{12}}{h'_2}\right) \quad (31)$$

For the case when the resolution point is reached within the column, $\theta_{feed} < \theta_{feed}^{RP}$, the band width is

$$\Delta\tau_{38} = \frac{z_{RP}}{U_3} - \tau_{RP} + \tau_{feed} \quad (32)$$

In terms of dimensionless time,

$$\Delta\theta_{38} = \frac{(1 + b_2 c_2^f + b_3 c_3^f - \alpha_{31} h'_2)\left(1 - \frac{\alpha_{12}}{h'_2}\right)}{(k'_2 - k'_3)\left(\frac{1}{K'_1} - \frac{1}{k'_2}\right)} \cdot \theta_{feed} \quad (33)$$

It is convenient to define displacement time, θ_{disp}, as the time for the displacer front to exit the column. It can be shown from eqns. 9, 23 and 12 that

$$\theta_{disp} = 1 + K'_1 \quad (34)$$

Column regeneration is an important consideration in the optimization of the displacement process. In this study, it has been assumed that the carrier is used as the regenerant. The wave generated in this process is diffuse [14] with boundary velocities

$$U_{slow} = \alpha_{41} \quad (35)$$

and

$$U_{fast} = (1 + b_1 c_1^f)^2 \alpha_{41} \quad (36)$$

The time required to complete the regeneration step, θ_{reg}, can be calculated, using eqn. 35, to be

$$\theta_{reg} = k'_1 \quad (37)$$

Note that the time required for regeneration is directly proportional to the elution capacity factor of the displacer.

The column throughput for product 2, that is, the amount of pure component 2 produced per unit time, is

$$TH = \frac{\Delta\theta c_2^{IS}}{\theta_{feed} + \theta_{disp} + \theta_{reg}} \quad (38)$$

This equation can now be used in combination with eqns. 29, 31 and 33 to optimize the operating parameters with respect to the throughput of component 2.

RESULTS AND DISCUSSION

For the purpose of studying the importance of various operating parameters on column throughput, the system shown in Table I was used, unless stated otherwise. It was assumed that component 2 is the desired product, but the approach is also applicable if both 2 and 3 are desired products. Further, for simplicity, the concentrations of 2 and 3 in the feed were assumed to be equal. The optimizations are based on a fixed column length, but an equivalent optimization based on a fixed feed time can also be performed.

Optimization of column loading

Effects of feed time. Feed time significantly influences the column response and separation performance. For displacement chromatography, when the feed time is small, a constant pattern or the isotachic condition is reached within the column, and the fully developed displacement train travels with no further separation, resulting in an inefficient use of the column and the displacer. Therefore, to

TABLE I

LANGMUIR COEFFICIENTS AND OPERATING PARAMETERS USED IN THIS STUDY

Parameter	Component		
	1 (displacer)	2	3
Langmuir coefficients			
k'	15	10	5
b (ml/mg)	0.1875	0.125	0.0625
Feed concentration, C (mg/ml)	15	2	2

increase the column utilization without increasing the displacer consumption, the feed time can be further increased such that the isotachic condition is just reached at the column exit. This is the case shown by the line A in Fig. 1, and corresponds to a feed time given by θ^{IS}_{feed}. Most displacement chromatographic separations have been operated below θ^{IS}_{feed}.

An increase in the feed time beyond θ^{IS}_{feed} results in non-attainment of the isotachic condition. This is represented by the region above line A in Fig. 1. However, although the isotachic condition is not reached, there is clearly a zone, between lines A and B, where complete separation is achieved. Hence a feed time greater than θ^{IS}_{feed} can be used for complete separation, further extending the utilization of the column.

If the feed time is increased beyond θ^{RP}_{feed}, incomplete separation of components 2 and 3 results. This corresponds to the region above line B in Fig. 1. The incomplete separation results in a lower recovery of pure component 2, and hence the throughput can be expected to decrease.

This dependence of column throughput on feed time was verified with the system of Table I using eqn. 38 in combination with eqns. 29, 31, 33, 34 and 37, and is shown in Fig. 2. For feed times less than θ^{RP}_{feed} a linear dependence between throughput and feed time was obtained. The throughput was maximum for $\theta_{feed} = \theta^{RP}_{feed}$, and decreased for larger feed times because of decreased recovery. The maximum throughput is, from eqn. 38,

$$TH_{max} = \frac{\theta^{RP}_{feed}\, c^{f}_{2}}{\theta^{RP}_{feed} + \theta_{disp} + \theta_{reg}} \qquad (39)$$

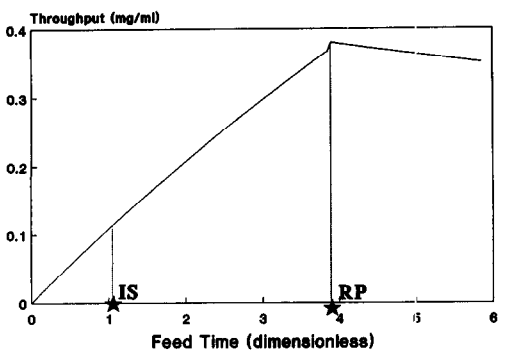

Fig. 2. Effects of feed time on throughput of component 2.

From Fig. 2 it can be seen that for a column loaded to θ^{RP}_{feed} the throughput of component 2 is close to four times larger than a column loaded to θ^{IS}_{feed}. Also, for feed times greater than θ^{RP}_{feed} the column is "overloaded". It should be noted that in all instances pure component 2 will be recovered at its isotachic concentration. However, total recovery of pure component 3 at its isotachic concentration can only be achieved if $\theta_{feed} \leqslant \theta^{IS}_{feed}$.

Optimum loading with non-ideal chromatographic behavior. The identification of θ^{RP}_{feed} as the optimum feed loading time was based on the assumption of ideal chromatography. In real systems, mass transfer resistances cannot be ignored. Mass transfer resistances will broaden boundaries, resulting in mixing between zones and, hence, lowered recoveries. As throughput will be affected, it is necessary to establish if the optimum feed loading criterion developed for ideal chromatography is valid in the non-ideal case.

In order to achieve this, displacement development was simulated for the system in Table I using an axial dispersion, linear driving force model [12]. The simulations were performed for a Peclet number of $1 \cdot 10^5$ and a range of Stanton numbers. Figs. 3–5 show chromatograms obtained for three feed times using a Stanton number of 200 in all instances. Fig. 3 is for a feed time of 1.05, θ^{IS}_{feed} for the ideal model, Fig. 4 is for a feed time of 3.89, θ^{RP}_{feed} for the ideal model, and Fig. 5 is for a feed time of 5.0. These and other simulations were used to calculate the throughput for component 2 of 98% purity, and the results are plotted in Fig. 6. It is clear that the dependence of throughput on feed time is very similar to the ideal

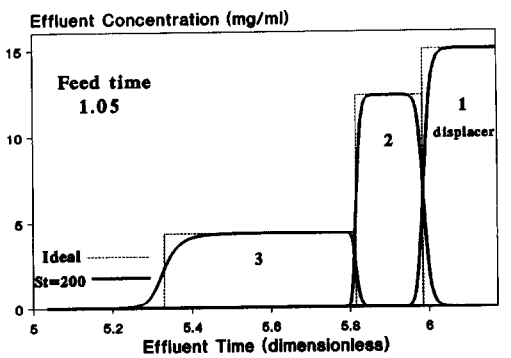

Fig. 3. Simulated displacement chromatogram at the isotachic capacity. $St = 200$; $Pe = 1 \cdot 10^6$.

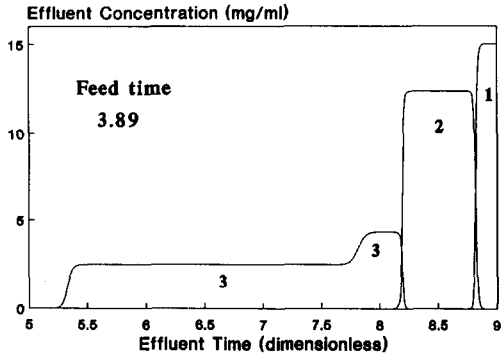

Fig. 4. Displacement chromatogram at the resolution capacity.

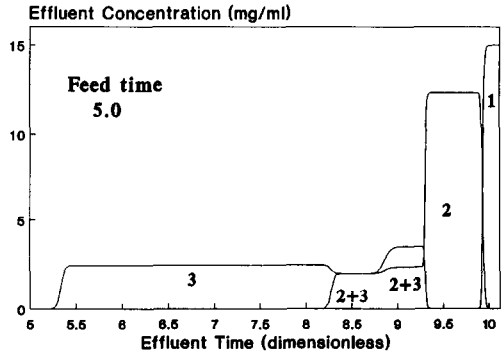

Fig. 5. Displacement chromatogram for column loading larger than its resolution capacity.

case. Although throughput decreases as the Stanton number increases, as is expected, in every instance θ_{feed}^{RP} obtained from the ideal case identifies the maximum throughput. This indicates that θ_{feed}^{RP} calculated from eqn. 24 can be used to optimize the column loading even when significant mass transfer resistances are present.

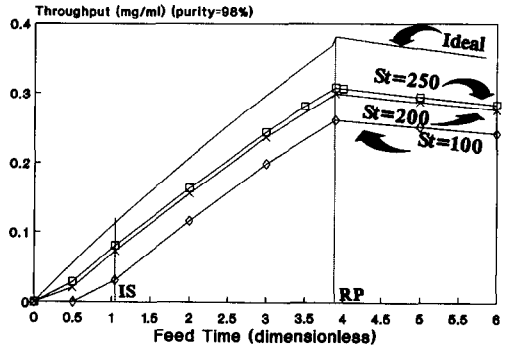

Fig. 6. Effect of non-ideality on column throughput.

In cases where mass transfer resistances or dispersion lead to significant overlap between adjacent zones in the displacement train, it is particularly important to optimize the feed loading. In Fig. 7 the recovery of component 2 (98% purity) is plotted as a function of feed time. It is clear that the θ_{feed}^{RP} provides the highest recovery. This can be easily understood from Figs. 3–5. For $\theta_{feed} < \theta_{feed}^{RP}$, as θ_{feed} increases the band width of the zones increases, and loss of useful products due to zone overlaps becomes less significant. Therefore, for example, operation at θ_{feed}^{IS} (Fig. 3) results in a lower recovery than operation at θ_{feed}^{RP} (Fig. 4). For $\theta_{feed} > \theta_{feed}^{RP}$ (Fig. 5), the separation of components 2 and 3 is not complete, which results in a lower recovery.

Also plotted in Fig. 7 is the total amount of product recovered as a function of feed time. Below θ_{feed}^{RP}, as the column is under-utilized, the amount recovered increases with increasing feed time. At and above θ_{feed}^{RP} the column is fully loaded, and the amount recovered remains constant. However, as θ_{feed}^{RP} represents the shortest feed time to attain the fully loaded condition, it gives the highest throughput.

Effects of feed concentration on throughput

It is well recognized that feed concentration has an important impact on the separation cost. For displacement chromatography, it is believed that the feed concentration should be as high as possible in order to load the sample at the top of the column. The effect of feed concentration on resolution capacity was investigated for the system in Table I. The effect of the total concentration of 2 and 3 was

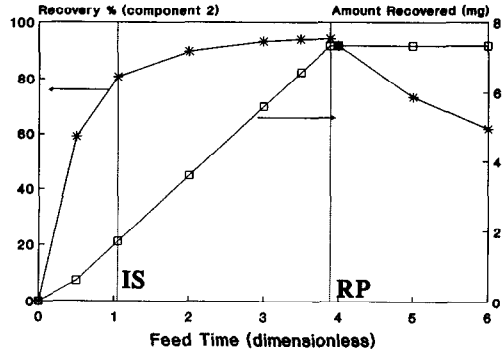

Fig. 7. Effect of column loading on recovery and amount recovered in non-ideal displacement chromatography. $St = 200$; $Pe = 1 \cdot 10^6$.

determined, keeping the displacer concentration constant. In all instances the concentrations of 2 and 3 were identical. The results of this study are shown in Fig. 8. The resolution capacity was initially found to decrease rapidly with increasing feed concentration. However, simultaneously, the maximum amount separated increased rapidly. Fig. 9 shows the cumulative effect on throughput. Throughput increases because for equal loadings the feed time decreases at higher feed concentrations.

An important feature of the dependence of throughput on feed concentration is the asymptotic approach to a maximum throughput. This has important implications in downstream processing. For dilute fermentation broths it is advantageous to concentrate the feed prior to a displacement separation. However, concentration beyond an optimum, determined by the economics of the displacement and concentration processes, may be counter-productive, as the gain in throughput will be insignificant.

Effects of properties of binary mixture on throughput

In this section only the effects of properties of the binary mixture will be considered, keeping the properties of the displacer constant. The effects of displacer properties will be discussed in the next section.

Separation factor. To study the effect of separation factor, α_{23}, on maximum column throughput, eqn. 24 was substituted into eqn. 39. Keeping all saturation capacities and k'_2 constant, the effect of α_{23} was obtained and is plotted in Fig. 10. At low values of the separation factor, the maximum

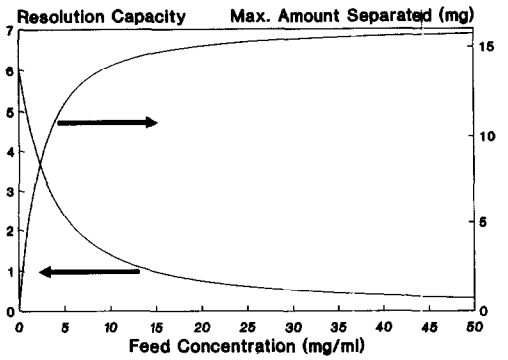

Fig. 8. Effect of feed concentrations on resolution and maximum amount separated.

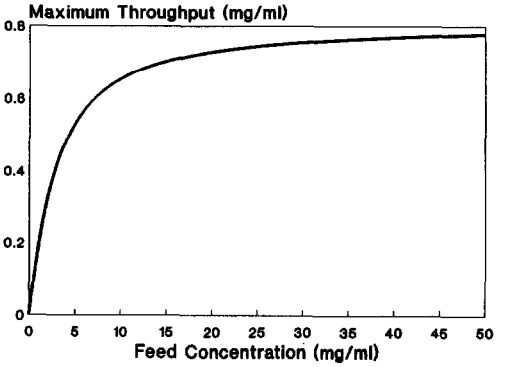

Fig. 9. Effect of feed concentrations on maximum column throughput.

throughput increases rapidly with increasing α_{23}. At high values of α_{23}, the behavior is asymptotic to an upper limit of the maximum throughput. Therefore, significant increases in separation factor will not in general translate into significant increases in throughput. Also, at low values of α_{23}, the throughput is proportional to $\alpha_{23} - 1$. This is in contrast to overloaded elution chromatography, where the throughput is proportional to $(\alpha_{23} - 1)^2$ [15]. Further, in the asymptotic region the throughput is approximately proportional to $(\alpha_{23} - 1)/\alpha_{23}$, which is similar to the dependence predicted by the resolution equation, eqn. 1, for elution chromatography. However, it should be noted that the relationship obtained is valid within the ideal model. For real columns, with limited efficiencies, the dependence of the throughput on the separation factor should be stronger [28].

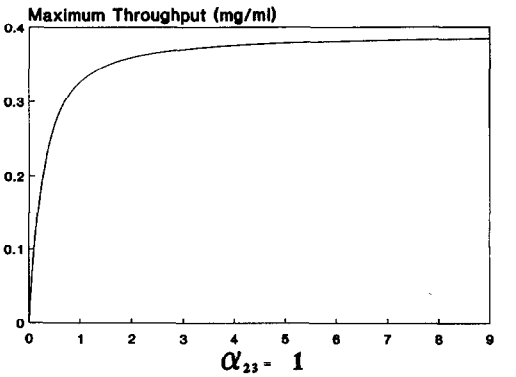

Fig. 10. Effect of separation factor on maximum column throughput.

Capacity factor. The effect of capacity factor on maximum throughput was also obtained by combining eqns. 24 and 39. In this instance, saturation capacities and separation factors were kept constant and both k'_2 and k'_3 were increased. The result is shown in Fig. 11. The maximum throughput was found to increase almost proportionally to k'_2, owing to the attainment of higher column loadings at higher capacity factors. This result is in contrast to elution chromatography, where optimum capacity factors are considered to be between 1.5 and 5. In elution chromatography, higher capacity factors result in longer separation times and hence lower throughputs. In displacement chromatography, however, the displacer velocity, not the capacity factors of the feed components, is the prime determinant of the separation time. Therefore, capacity factors should be as large as possible in order to maximize the throughput, within the limitation that these capacity factors are less than the capacity factor of the displacer.

Saturation capacity. The effect of saturation capacities on the maximum throughput was also studied by substituting eqn. 24 into eqn. 39. As the saturation capacities are $k'_i/\phi b_i$, the b_i values were systematically varied keeping all other parameters constant. Identical saturation capacities were used for components 2 and 3. The effect observed (Fig. 12) is similar to the effect of feed concentration and separation factor, with a strong dependence at low saturation capacities and asymptotic behavior at high saturation capacities. At low values the maximum throughput is small owing to the limited loading capacity, although the displacement effect is

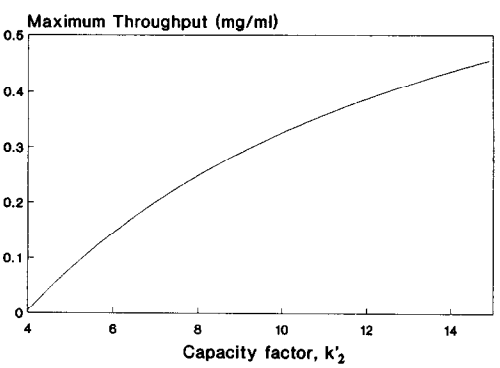

Fig. 11. Effect of capacity factors on maximum column throughput.

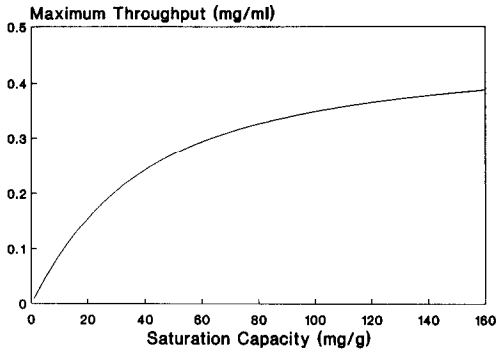

Fig. 12. Effect of saturation capacity on maximum column throughput.

pronounced [29]. This result indicates that nonporous supports, normally of low saturation capacity, are not suitable for displacement chromatography, although they may have more favorable mass transfer characteristics. Also, as low saturation capacities may result from a high modulator concentration, it is important to optimize the type and concentration of modulator used.

Effects of displacer on column throughput

Minimum displacer concentration. With reference to Fig. 1, the first requirement for a successful displacement separation of components 2 and 3 is that U_5 should be larger than U_1. From eqns. 10 and 14, this requires a minimum displacer concentration such that

$$K'_1 < k'_2 \tag{40}$$

This condition is consistent with the requirement that θ^{RP}_{feed} should be positive (eqn. 24). Attainment of the isotachic condition further requires that U_7 must be larger than U_2 (Fig. 1). This requires that

$$K'_1 < k'_3 \tag{41}$$

When only eqn. 40 is satisfied, component 3 is eluted and component 2 is displaced. The conditions given by eqns. 40 and 41 are represented in Fig. 13. Note that these conditions require that the slope of the operating line be less than the slope at infinite dilution of the isotherms of the mixture components, a well known condition for displacement chromatography [2].

Effects of displacer concentration on throughput. The effect of displacer concentration on throughput

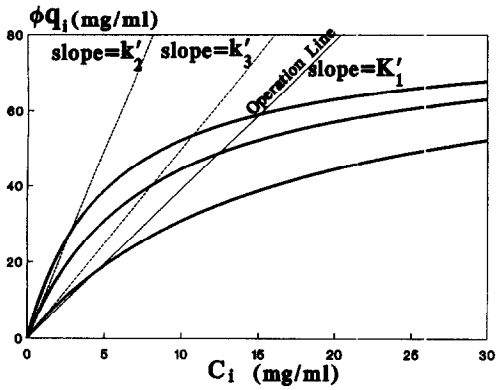

Fig. 13. Displacer and feed adsorption isotherms and operation line.

was determined from eqns. 25, 34 and 39, and is shown in Fig. 14. At low concentrations, significant gains can be made with regard to the throughput by increasing displacer concentration. However, at higher concentrations the dependence of throughput on displacer concentration is weak. This weak dependence is due to small frontal capacity factors at high concentrations (eqn. 25), which makes θ_{disp} almost independent of concentration (eqn. 34). Hence the maximum throughput (eqn. 39) is only weakly influenced. The weak influence at high concentrations indicates that a higher displacer concentration may not always be economically favored. Also, it should be noted that the highest displacer concentration that can be used in practice may be limited by solubility and mass transfer considerations [12,30].

Displacer optimization. A requirement in the selection of a displacer is that the displacer affinity be higher than that of any of the components in the mixture. However, displacer affinity also influences the column regeneration (eqn. 37) and, hence, column throughput. As displacers with the same value of K'_1 will give the same displacement separation for a given mixture, it is possible to reduce θ_{reg} without affecting the displacement separation. From eqn. 25, a reduction in k'_1 can be compensated for by a change in the feed concentration c_1^f. This is illustrated on the operating diagram in Fig. 15 for three displacers 1, 1′ and 1″. As an example, displacers 1 and 1″ would give the same separation if displacer concentrations of c'_1 and c''_1 were used, respectively. However, as 1″ has a lower k'_1 value, the regeneration would be quicker with this displacer. This analysis indicates that a displacer with b_1 values as small as possible and with k'_1 values close to the affinities of the desired components should be selected for maximum throughput.

The importance of optimizing displacer affinity with respect to both column development and regeneration has recently been demonstrated for the ion-exchange displacement chromatography of proteins [7,8]. It has been shown that lower affinity polyelectrolyte displacers can be used effectively for displacement development, and they are more efficiently removed from the column during regeneration than analogous higher affinity displacers. This is consistent with the conclusions reached above.

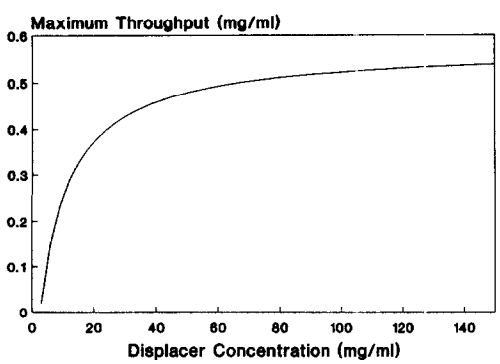

Fig. 14. Effect of displacer concentration on maximum column throughput.

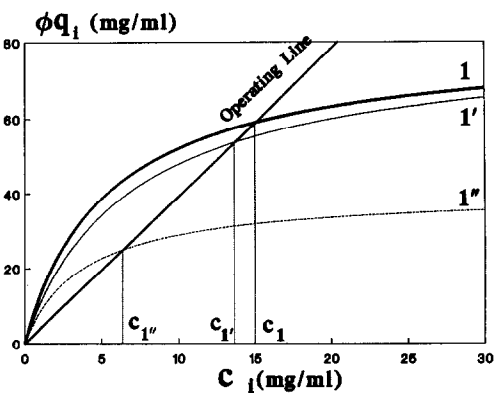

Fig. 15. Effects of concentration and affinity on displacer frontal capacity.

Simple method for determination of maximum column loading

For practical applications, it is very useful to establish a simple procedure for determining θ^{RP}_{feed} and θ^{IS}_{feed}. This can be done with two sets of experiments. An elution chromatographic separation should be performed with a sample concentration low enough to ensure no interference between components. From these data, the elution capacity factors can be calculated

$$k'_i = \frac{t_i - t_0}{t_0} \tag{42}$$

The frontal capacity factor, K'_{im}, defined as

$$K'_{im} = \frac{T_{im} - T_0}{T_0} \tag{43}$$

is obtained from a frontal injection of the sample at its feed concentration.

These capacity factors can be used to calculate required h compositions [27]. For binary mixtures,

$$\alpha_{31} h'_2 = \frac{K'_{3m}}{K'_{2m}} \quad \text{and} \quad \alpha_{31} h'_3 = \frac{k'_3}{K'_{3m}} \tag{44}$$

Also, it has been shown [27] that

$$K'_{2m} = \frac{k'_2}{1 + b_2 c_2^f + b_3 c_3^f} \tag{45}$$

Substituting eqns. 44 and 45 into eqns. 24 and 28, θ^{RP}_{feed} and θ^{IS}_{feed} are obtained in terms of the measured parameters:

$$\theta^{RP}_{feed} = \frac{1 - \dfrac{k'_3}{k'_2}}{\dfrac{k'_2}{K'_{2m}} - \dfrac{K'_{3m}}{K'_{2m}}} (k'_2 - K'_1) \tag{46}$$

and

$$\theta^{IS}_{feed} = \frac{\left(1 - \dfrac{K'_1}{k'_2}\right)\left(\dfrac{k'_3}{K'_1} - 1\right)}{\dfrac{k'_3}{K'_{3m} K'_1} - \dfrac{1}{K'_{2m}}} \tag{47}$$

It is interesting that with very dilute feed samples K'_{im} approaches k'_i, and eqns. 46 and 47 reduce to

$$\theta^{RP}_{feed} = k'_2 - K'_1 \quad \text{and} \quad \theta^{IS}_{feed} = k'_3 - K'_1 \quad \text{as} \quad c_i^f \to 0 \tag{48}$$

These correspond to the maximum feed times for the resolution and isotachic conditions, respectively. For complete resolution, the maximum feed time is simply the difference between the infinite dilution slope of the isotherm of the more retained component and the slope of the operating line for the displacement process (Fig. 13). Similarly, for the isotachic condition, the maximum feed time is given by the difference between the infinite dilution slope of the less retained component and the slope of the operating line.

Extension to multi-component mixtures

The procedure developed here for a binary mixture can be extended to multi-component systems in most instances. Fig. 16 shows the distance–time diagram for displacement chromatography of a ternary mixture. For this case, there are two resolution points and one isotachic point. Similarly, for an n-component mixture, there are $n - 1$ resolution points and one isotachic point. The optimum loading will depend on the desired component. For an n-component system with the displacer as the highest affinity component, the maximum throughput occurs at the ith resolution point if the desired product is the ith component.

If $h'_{n+1} < 1 + b_1 c_1^f$, then all the waves generated are sharp, and all the resolution and isotachic points can be calculated as a function of separation factors and the h-root compositions of the feed. Further, these h-roots can be expressed in terms of the frontal and elution capacity factors [27]. The capacity factors can be calculated from eqns. 42 and 43. In cases where diffuse waves are generated in an n-component displacement, this method is still ap-

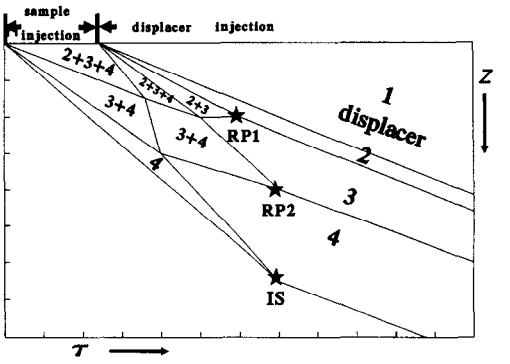

Fig. 16. Simplified distance–time diagram for the displacement chromatography of ternary separations.

plicable for the calculation of the resolution points, but not for the isotachic point. The generation of diffuse waves can be predicted from

$$K'_{n+1,m} > K'_1 \tag{49}$$

Finally, a similar methodology can be applied to the determination of the maximum feed time in overloaded elution chromatography.

CONCLUSIONS

The coherence theory provides a general and convenient framework for the optimization of displacement chromatography. Using this framework, it has been shown that throughput for a binary separation is maximized when the column is operated at the resolution point. Further, the result appears to be valid when mass transfer and/or axial dispersion effects are significant. Therefore, the optimum column loading is almost independent of the column efficiency, and the recovery and column efficiency will be traded in a compromise maximizing the throughput.

The effects of feed concentration, separation factor, saturation capacities and displacer concentration on the throughput have also been determined. Larger values of all these parameters give higher throughputs. However, in each instance the optimum value will not, in general, be the highest value of the parameters, because of an asymptotic dependence of throughput on these parameters. With regard to the capacity factor of the desired component, k'_2, and the displacer, k'_1, a high value of k'_2 and a low value of k'_1 are desired. A high value of k'_2 enhances column loading, and a low value of k'_1 is advantageous with respect to column development, regeneration and displacer solubility. However, the lowest value of k'_1 is limited by the affinity of the most strongly retained component in the mixture.

This optimization method, developed here for a binary mixture, can be extended to multi-component systems. In this instance, if the ith component is the desired product, the maximum throughput will be established by the ith resolution point, that is, the point on the distance–time diagram where the ith component is completely separated from the remainder of the mixture.

Finally, the use of the compound Langmuir model in this study places restrictions on its applications to the systems deviating markedly from Langmuir behavior.

ACKNOWLEDGEMENT

This work was supported in part by Grant No. CTS-8909742 from the National Science Foundation. This support is gratefully acknowledged.

SYMBOLS

a_i	affinity constant, Langmuir parameter of adsorbate i
b_i	Langmuir parameter of adsorbate i
c_i	mobile phase concentration of adsorbate i
c_i^f	feed concentration of adsorbate i
c'_1	required concentration of the displacer, 1′, in Fig. 15
c''_1	required concentration of the displacer, 1″, in Fig. 15
h	h-root
h'_i	h-root of frontal injection of the binary mixtures
k'_i	elution capacity factor of adsorbate i at the infinite dilution, $k'_i = \phi a_i$
k'_4	elution capacity factor of the dummy species
K'_1	frontal capacity factor of the displacer
K'_{im}	frontal capacity factor of ith component in frontal chromatography of the binary mixture
L	column length
n	number of adsorbates
N	number of theoretical plates
Pe	Peclet number, product of interstitial velocity and column length divided by effective axial dispersion coefficient
q_i	average stationary phase concentration of adsorbate i
q_i^*	equilibrium stationary phase concentration of adsorbate i
Q_i	$Q_i = \phi q_i$
Q_i^*	$Q_i^* = \phi q_i^*$
St	Stanton number, product of mass transfer rate and column length divided by interstitial velocity
t	real time
t_0	column hold-up time in elution chromatography

t_i retention time of adsorbate i in linear isocratic elution chromatography
T_0 column hold-up time in frontal chromatography
T_1 breakthrough time in frontal or displacement chromatography of the displacer
T_{im} retention time of the ith component in frontal chromatography of the binary mixture
TH throughput (amount of product produced per unit of time) divided by the column flow-rate
TH_{max} maximum value of TH, occurring at the resolution point
u_0 interstitial bulk phase velocity
u_i true velocity of adsorbate i
U_i adjusted velocity of adsorbate i
z column distance

Greek letters

α separation factor
ϕ column phase ratio
θ dimensionless time (t/t_0)
θ_{feed} dimensionless feed time (or column loading) for injection of the binary mixture
θ_{feed}^{IS} maximum dimensionless feed time with which the isotachic condition can be achieved
θ_{feed}^{RP} maximum dimensionless feed time with which the complete separation is possible
τ adjusted time (unit of length)

REFERENCES

1 B. J. Spalding, *Bio/Technology*, 9 (1991) 229–233.
2 J. Frenz and Cs. Horváth, in Cs. Horváth (Editor), *High-Performance Liquid Chromatography —Advances and Perspectives*, Vol. 5, Academic Press, New York, 1988, pp. 211–314.
3 S. M. Cramer and G. Subramanian, *Sep. Purif. Methods*, 19 (1990) 31–91.
4 H. Colin, in P. R. Brown and R. A. Hartwick (Editors), *High-Performance Liquid Chromatography*, Wiley, New York, 1989, p. 415.
5 G. Subramanian and S. M. Cramer, *Biotechnol. Prog.*, 5 (1989) 92.
6 A. M. Katti, E. V. Dose and G. Guiochon, *J. Chromatogr.*, 540 (1990) 1–20.
7 S.-C. D. Jen and N. G. Pinto, *J. Chromatogr. Sci.*, 27 (1991) in press.
8 S.-C. D. Jen and N. G. Pinto, *J. Chromatogr.*, 519 (1990) 87–98.
9 N. B. Afeyan, N. F. Gordon, I. Mazsaroff, L. Varady, S. P. Fulton, Y. B. Yang and F. E. Regnier, *J. Chromatogr.*, 519 (1990) 1–29.
10 J. M. Miller, *Chromatography: Concepts and Contrasts*, Wiley, New York, 1988.
11 G. K. Sofer and L. E. Nyström (Editors), *Process Chromatography: a Practical Guide*, Academic Press, San Diego, 1989.
12 M. W. Phillips, G. Subramanian and S. M. Cramer, *J. Chromatogr.*, 454 (1988) 1–21.
13 T. Gu, G.-J. Tsai and G. T. Tsao, *Biotechnol. Bioeng.*, 37 (1991) 65–70.
14 F. Helfferich and G. Klein, *Multicomponent Chromatography: Theory of Interference*, Marcel Dekker, New York, 1970.
15 S. Golshan-Shirazi and G. Guiochon, *Anal. Chem.*, 61 (1989) 1276.
16 H.-K. Rhee and N. R. Amundson, *AIChE J.*, 28 (1982) 423–433.
17 F. Helfferich and D. B. James, *J. Chromatogr.*, 46 (1970) 1–28.
18 J. Frenz and Cs. Horváth, *AIChE J.*, 31 (1985) 400–409.
19 A. M. Katti and G. Guiochon, *J. Chromatogr.*, 449 (1988) 25–40.
20 S. Golshan-Shirazi and G. Guiochon, *J. Chromatogr.*, 545 (1991) 1–26.
21 F. Antia and Cs. Horváth, paper presented at the *8th International Symposium on Preparative Chromatography, PREP '91*, Washington, DC, May, 1991.
22 D. B. Broughton, *Ind. Eng. Chem.*, 40 (1948) 1506.
23 C. Kemball, E. K. Rideal and E. A. Guggehnheim, *Trans. Faraday Soc.*, 44 (1948) 952.
24 G. B. Cox and L. R. Snyder, *J. Chromatogr.*, 483 (1989) 95–110.
25 E. C. Markham and A. F. Benton, *J. Am. Chem. Soc.*, 53 (1931) 497.
26 J. M. Jacobson and J. Frenz, *J. Chromatogr.*, 499 (1990) 5–19.
27 S.-C. D. Jen and N. G. Pinto, presented at the *8th International Symposium on Preparative Chromatography, PREP'91*, Arlington, VA, May, 1991.
28 G. B. Cox and L. R. Snyder, *J. Chromatogr.*, 483 (1988) 95–110.
29 T. Gu, G. T. Tsao, G.-J. Tsai and M. R. Ladisch, *AIChE J.*, 36 (1990) 1156–1162.
30 J. Frenz, P. van der Schriek and Cs. Horváth, *J. Chromatogr.*, 330 (1985) 1–17.